

may be seen that we have reduced the  $\tau_0$  cofactor in eq 1 also by more than 2, yet  $\tau_c$  has remained unchanged. We conclude that the kink process, rather than viscous drag on the surface of the helices, controls high-frequency motion in these polymers.

That there is a qualitative difference between the behavior of the terpolymers when  $x = 0$  (motional narrowing conditions apply) and when  $x = 1$  and 0.92 (motional narrowing conditions do not apply) indicates there is a distinct difference in chain dynamics: the simple conclusion obtained above does not thus depend solely upon the use of the anisotropic single  $\tau_c$  model for interpreting  $T_1$  values. (We note also that the stiff sections in such terpolymers may not be perfectly isotropic helices.<sup>4</sup>) Assuming that the *cis*-but-2-ene sulfone units, when isolated in the mainly but-1-ene sulfone chain, interrupt the configurational order as do the cyclohexene units in the mainly hex-1-ene sulfone chain,<sup>1,4,5</sup> we can understand the absence of kinetic freedom from the present terpolymer in the following terms: we suppose that in the 1-olefin sulfone homopolymer the kink, created by a *trans* C-C bond, is capable of moving from one site to the next along the chain so that helix rotation is coupled to kink translation. On the other hand, *trans* C-C bonds created by the inclusion of isolated but-2-ene sulfone units cannot escape from their site in such a chain and thus cannot introduce further kinetic flexibility. It remains possible that a process not included in our simple model of eq 1, such as high-frequency local librations, is responsible for the magnetic

relaxation within the stiffer 1-olefin sulfone sections.

**Acknowledgment.** S.A.C. thanks the Arbutnot fund for support during part of this work. We both thank Dr. L. C. Waring for recording the spectra.

## References and Notes

- (1) Fawcett, A. H.; Fee, S. *Macromolecules* **1982**, *15*, 933.
- (2) Matsuo, K.; Mansfield, M.; Stockmayer, W. H. *Macromolecules* **1982**, *15*, 935.
- (3) Mansfield, M. *Macromolecules* **1982**, *15*, 1587.
- (4) Cole, R. H.; Fawcett, A. H.; Fee, S.; Winsor, P., to be submitted.
- (5) Fawcett, A. H.; Fee, S.; McKee, S. G.; Quigg, R. K. "Abstracts of Communications", 27th International Symposium on Macromolecules, Strasbourg, July 1981, Vol. II, p 616.
- (6) Cais, R. E.; Bovey, F. A. *Macromolecules* **1977**, *10*, 757.
- (7) Fawcett, A. H.; Heatley, F.; Ivin, K. J.; Stewart, C. D.; Watt, P. *Macromolecules* **1977**, *10*, 765.
- (8) Bovey, F. A. In "Stereodynamics of Polymer Systems"; Sarma, R. H., Ed.; Pergamon: Oxford, 1979; Bovey, F. A.; Cais, R. E. "Carbon-13 in Polymer Science"; Pasica, W. A., Ed.; "ACS Symp. Ser."; American Chemical Society: Washington, DC, 1979; No. 103.
- (9) Fawcett, A. H.; Fee, S.; Waring, L. C. *Polymer* **1983**, *24*, 1571.
- (10) Chambers, S.; Fawcett, A. H., to be submitted.
- (11) Fawcett, A. H.; Ivin, K. J.; Stewart, C. D. *Organ. Magn. Reson.* **1978**, *11*, 360.
- (12) We use the relationship for  $\tau_c$  suitable for a body rotating about a fixed axis: Debye, P. "Polar Molecules"; The Chemical Catalog Co., 1929, p 96.
- (13) We ignore the small proportion of but-1-ene units at a kink that might be more mobile.
- (14) Hazell, J. E.; Ivin, K. J. *Trans. Faraday Soc.* **1962**, *58*, 176.
- (15) Fawcett, A. H.; Ivin, K. J. *Polymer* **1972**, *13*, 439.

## Dynamical Properties of High Molecular Weight Polystyrene in Tetrahydrofuran in the Dilute-Semidilute Transition Region

Wyn Brown

*Institute of Physical Chemistry, University of Uppsala, 751 21 Uppsala, Sweden.  
Received November 16, 1984*

**ABSTRACT:** Data are presented for the polystyrene ( $M = 8 \times 10^6$  and  $M = 15 \times 10^6$ )-tetrahydrofuran system, which has been probed by dynamic light scattering in the  $1 < qR < 4$  region at  $C/C^* \leq 200$ . Measurements on the same system were also made by classical gradient diffusion. In dilute solutions the correlation functions were fitted to a bimodal expression to allow evaluation of the first internal mode  $\tau_1$  and the translational diffusion coefficient.  $\tau_1$  is found to be in approximate agreement with the value given by Zimm's nondraining model. Bimodal autocorrelation functions are also found to typify the semidilute region well above  $C^*$  and in a region where unimodal behavior is predicted by de Gennes' theory and are attributed to a composite of fast and slow cooperative modes over the concentration range investigated. It appears unlikely that experimental parameters can be chosen to allow *direct* characterization of a unique pseudogel mode. Such composite character, which appears to be generally valid with samples of very high molecular weight, severely restricts the use of photon correlation spectroscopy for testing models of the semidilute region which are formulated in terms of a specific relaxational mode.

## Introduction

Above the critical concentration for overlap of individual polymer coils,  $C^*$ , the dynamical structure factor,  $S(q,t)$  is predicted<sup>1</sup> to be related to a collective mode which characterizes the transient network formed by intermolecular entanglements. Using photon correlation spectroscopy (PCS) the range of  $q\xi$  values where the dynamics of the transient gel should be observable will be wide at high values of  $(C/C^*)$  and lie between

$$(C/C^*)^{-1.125} < q\xi < (C/C^*)^{0.75}$$

Here,  $q$  is the scattering vector and  $\xi$  is a dynamic correlation length of the concentration fluctuations. Between

the above bounds the autocorrelation function was predicted to decay exponentially and one can thus define a unique collective diffusion coefficient:

$$D_c = kT/6\pi\eta_0\xi \quad (1)$$

where  $k$  is Boltzmann's constant,  $T$  is the absolute temperature, and  $\eta_0$  is the solvent viscosity. The first experimental tests of the above were those of Daoud et al.<sup>2</sup> using neutron scattering and of Adam and Delsanti<sup>3</sup> with PCS measurements on PS/benzene. In the so-called "pseudogel domain" the latter concluded that  $S(q,t)$  was a single-exponential function of time. The inverse relaxation time ( $\bar{\Gamma}$ ) was found to be  $q^2$  dependent and  $\Gamma \sim C^{0.67}$ , in ap-

proximate agreement with the predicted value of 0.75. There is, however, an accumulated body of evidence which conflicts in essentials with these findings. The time correlation function for semidilute solutions in both good and poor solvents is frequently reported to be nonexponential<sup>4-14</sup> and this feature shows a systematic variation with both concentration and scattering angle. Several groups<sup>4-6,9-12</sup> have employed routines for bimodal analysis. One can in this way resolve the autocorrelation function into a fast (pseudogel) mode and a slower (possibly hydrodynamic) component. An example is provided by the investigations of Chu and Nose<sup>4</sup> of the PS/*trans*-decalin  $\theta$  system. They demonstrated the participation of two competing modes throughout the semidilute region. The relative intensity contributions were found to depend on the location in the  $q\xi$ -( $C/C^*$ ) plane. Nishio and Wada<sup>6</sup> came to similar conclusions on studying the PS/2-butanone system, which involves a marginal solvent. It is also relevant that Yu et al.<sup>5</sup> found it necessary to modify the relaxation diagram of de Gennes<sup>1</sup> in order to accommodate a broad transition region with bimodal character and used it to interpret data for the PS/THF system. The generality of the presence of multiple relaxations in PCS experiments has not hitherto been emphasized, however. It is only exceptionally that one can choose experimental parameters to exclude all relaxational modes except the one of interest at semidilute concentrations. This work is directed toward elucidation of the extent to which, in particular, the pseudogel behavior can be experimentally characterized with PCS. In order to address this question it is necessary to make precise measurements on a high molecular weight, narrow-distribution polymer in a good solvent. The measurements are further to be made in the  $q\xi$ -( $C/C^*$ ) region in which one anticipates from theory that a single mode will be in evidence. Over the concentration range below and close to  $C^*$ , the approximation  $\xi = R$  is made,  $R$  being the radius of gyration. The value of  $R$  in THF is assumed here to equal that in benzene, another good solvent, for which a relationship is given in ref 3. We use here the definition  $C^* = 3M/4\pi R^3 N_A$ .

The present paper mainly describes measurements on a polystyrene ( $M = 8 \times 10^6$ ), essentially monodisperse, in the thermodynamically good solvent THF. A range of angles is employed spanning the region  $1 < qR < 4.5$  and with concentrations extending up to a reduced value of  $(C/C^*) \leq 200$ . The results are initially treated with a cumulants fit. Subsequently, the data treatment is made using a three-parameter model, a four-parameter model, and also the latter with inclusion of a base-line term. The data are compared with measurements made with the classical concentration gradient technique.

## Experimental Section

**Materials.** Narrow-distribution polystyrene ( $M = 8 \times 10^6$ ,  $M_w/M_n = 1.08$ , and  $M = 15 \times 10^6$ ,  $M_w/M_n = 1.30$ ) were obtained from Toya Soda Ltd., Tokyo, Japan. THF was spectroscopic grade from Merck, Darmstadt, FRG, and was used without further purification.

**Solutions** were prepared in sealed glass vials, allowed to rotate/precess at 1 rev/min for approximately 2 months at 25 °C. The contents were then very slowly filtered through 3.0- $\mu$ m Fluoropore filters in a closed-circuit filtration apparatus. After two (usually) passes, the filtrate was bled off into weighed 10-mm-diameter precision NMR tubes and reweighed. In order for a bimodal analysis (or indeed any multiexponential analysis) of the time correlation function to be meaningful, it is imperative for interpretation that there is no background scattering from dust or other nonhomogeneity. Dilutions were performed by filtering various amounts of solvent into the tubes. A series of solutions of high optical quality were obtained in the range 0.01–1% (w/w). Solutions were allowed to stand for several weeks

before measurement. Higher concentrations were then prepared by very slow evaporation of solvent from a known amount of stock solution in the light scattering tubes in a dust-free atmosphere.

**Photon Correlation Spectroscopy.** The experimental arrangement has been summarized recently.<sup>12</sup> Measurements were made in the angular range  $\theta = 20$ – $80^\circ$  ( $qR = 1$ – $4.5$ ) with the NMR tubes immersed in a large-diameter bath of index-matching liquid (decalin). All experiments were performed in the homodyne mode; see ref 12 for further details. Incident radiation at 488 nm was provided by a Coherent CR-4 argon ion laser containing a quartz etalon frequency stabilizer in the cavity to ensure single-mode operation and enhance the signal/noise ratio. The data were collected with a Langley-Ford 128-channel full correlator coupled to a Luxor ABC-800 microcomputer for data collection and reduction.

**Classical gradient diffusion** measurements were made as described recently,<sup>12</sup> using a shearing-type cell and a schlieren optical system. The boundary was always made between solutions differing in concentration by not more than 1%. The starting-time correction was always zero within experimental error; the run was otherwise rejected.

**Data treatment** has been described in some detail in a previous communication.<sup>12</sup>

The quality of the data has been substantially improved over that of the earlier investigation<sup>12</sup> through use of an automatic data collection procedure. With the latter, approximately 60–80 runs, each of length 1 s, are accumulated using minimization of the total intensity and added together for each set of measurement parameters. Thus a comparison of the mean value of the total intensity per second ( $I$ ) of each run is made with the preceding run. If it lies within  $\pm 4\%$  it is accepted; if higher the run is rejected. If outside this range and lower, all earlier runs are rejected and a new set of runs is accumulated relative to the new intensity standard until at least 60 runs falling within  $\pm 4\%$  have been assembled.

This procedure has substantially eliminated any extraneous contributions to the total intensity and gives data with a variance improved by at least an order of magnitude compared with manual operation of the correlator. The statistical base line (i.e., total pulse times mean pulses per sampling time) was of the order  $2 \times 10^7$ . Only runs in which the statistical base line agreed closely with the value from the delayed channels were used. All data were initially processed by a cumulant fit program using a third-order cumulant fit. Runs exhibiting deviant intensity were rejected. The fits were based on points 3–128 in order to eliminate distortions in the first channels from after pulsing. Measurements at semidilute concentrations were restricted to the angular region showing no significant trend in  $\bar{D}_{cum}$  with measuring angle in order to avoid contamination from internal motions. Bimodal fits were made by using an equally weighted, nonlinear regression procedure according to Marquardt.<sup>32</sup>

Some workers use an adjustable base line, the origin of which is attributed to long-term laser drift and/or a dust background. We have been unable to detect laser drift and using a continuous filtering technique are able to prepare consistently dust-free solutions. We can thus fix the base line in conjunction with use of eq 2 below. A number of simulated experiments were made to evaluate the reliability of the calculation procedure. Bimodal fits were made according to the function

$$g^{(2)}(\tau) - 1 = \beta[A_s \exp(-\Gamma_s \tau) + A_f \exp(-\Gamma_f \tau)]^2 \quad (2)$$

Figure 1 shows the residuals for a typical bimodal fit vs. channel number and scaled in standard deviations. These data are for 0.16% (w/w). The parameter  $\beta = 0.69$ ,  $A_s = 0.62$ ,  $\Gamma_s = 1.21 \times 10^3 \text{ s}^{-1}$ ,  $A_f = 0.38$ , and  $\Gamma_f = 4.6 \times 10^3 \text{ s}^{-1}$ .

## Results and Discussion

The results described in this section extend from the dilute through the semidilute ranges of concentration. Figures 2 and 3 show, respectively, plots of inverse relaxation times ( $\Gamma$ ) as a function of the square of the scattering vector,  $q$ . The two curves in each diagram correspond to the fast ( $\Gamma_f$ ) and slow ( $\Gamma_s$ ) components of the time correlation function, for the concentrations shown, resolved with bimodal fits according to eq 2. Bimodal fits were preferred

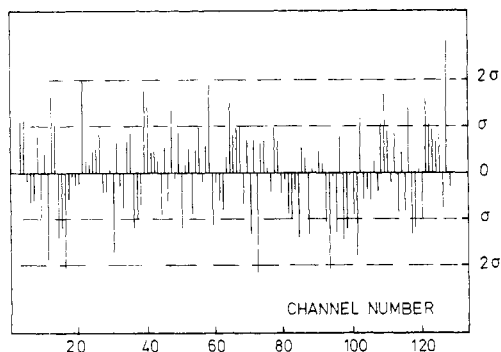


**Figure 1.** Plot of residuals for a typical experiment vs. channel number where a bimodal fit has been employed. ( $C = 0.16\%$  (w/w); angle =  $60^\circ$ ).

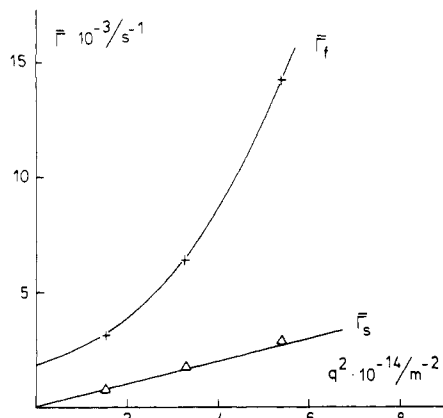


**Figure 2.** Relaxation frequency vs. square of scattering vector for dilute solution data using eq 2 to evaluate  $\bar{\Gamma}_f$  and  $\bar{\Gamma}_s$  (see eq 4 and 5). Data for PS ( $M = 8 \times 10^6$ );  $C = 0.021\%$  in THF.

in the present systems over three-parameter fits (i.e., single exponential plus floating base line) on the basis of the  $Q$  function:

$$Q = 1 - \frac{\sum_{i=1}^{n-1} \epsilon_i \epsilon_{i+1} / n - 1}{\sum_{i=1}^n \epsilon_i \epsilon_i / n} \quad (3)$$

If there is no grouping of residuals,  $\epsilon$ ,  $Q$  will approximate unity; otherwise  $Q$  will be significantly less than one.  $Q$  values of approximately unity were consistently obtained for fits using eq 2 for data at all but the lowest angles at dilute concentrations (see also Figure 6a) whereas a three-parameter fit gave  $Q \lesssim 0.5$ . The addition of a fifth term (base line) to eq 2 was found to lack statistical significance on the basis of the minimization of the reduced sum of squares of residuals,  $\chi^2$ .

In Figure 2 the inverse relaxation time of the slower component is linear in  $q^2$  and the slope may be identified with translational diffusion of the whole coil. The value of  $D_0$  obtained by extrapolation to infinite dilution agrees well with the value for this molecular weight derived from the  $\log D - \log \bar{M}_w$  relationship given in ref 16. At low angles ( $\theta \leq 20^\circ$ ) corresponding to  $qR < 1$  the correlation function is unimodal. With increasing angle it becomes bimodal. Both the translational mode and a composite of higher modes are then represented in the correlation function. With this as starting point, several groups<sup>17-21</sup> have shown that it is possible to evaluate the longest internal relaxation time,  $\tau_1$ .

Thus, a collective intramolecular relaxation is measurable at finite  $q$ , while as the intercept at  $q \rightarrow 0$  one obtains

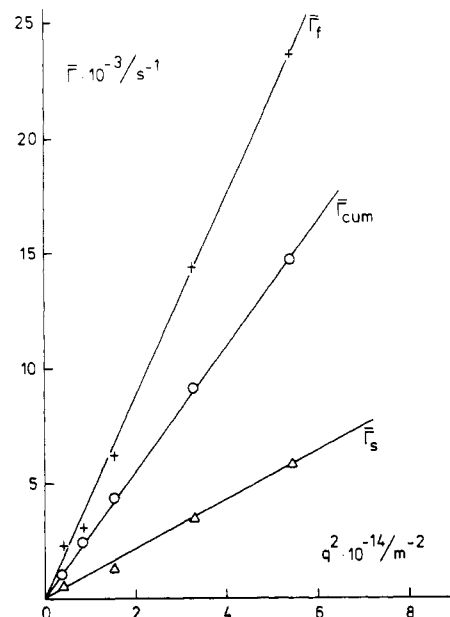


**Figure 3.** Bimodal analysis (eq 2) results for a semidilute solution ( $C = 0.86\%$ ) of PS ( $M = 8 \times 10^6$ ) in THF.  $\bar{\Gamma}_f$  and  $\bar{\Gamma}_s$  correspond to fast and slow cooperative relaxations.  $\bar{\Gamma}_{cum}$  are points from cumulant analysis.<sup>15</sup>

half the relaxation time of the lowest mode,  $\tau_1$ , according to

$$\bar{\Gamma}_f = (q^2 D + 2/\tau_1)_{q \rightarrow 0} \quad (4)$$

and

$$\bar{\Gamma}_s = q^2 D \quad (5)$$

$\bar{\Gamma}_f$  is difficult to obtain by extrapolation with precision owing to its very low intensity amplitude at low angles. Since, however,  $(\bar{\Gamma}_f - \bar{\Gamma}_s)$  is found to be approximately independent of concentration in the dilute range, we have evaluated  $\tau_1$  from  $(\bar{\Gamma}_f - \bar{\Gamma}_s) = 2/\tau_1$  by averaging data at three dilute concentrations at low angles. The value  $\tau_1 \approx 1 \times 10^{-3}$  s was obtained. Since emphasis in this paper is on the semidilute region, the value of  $\tau_1$  is given here as a good estimate only. Following Jones and Caroline,<sup>19</sup> the value of  $\tau_1$  can also be estimated from the relationship

$$\tau_1 = M\eta_0[\eta]/A_1 R T \quad (6)$$

where  $A_1$  is 0.822 for the Rouse<sup>34</sup> bead-spring free-draining model and 1.18 for the Zimm<sup>33</sup> nondraining model.  $M$  is molecular weight,  $\eta_0$  is the solvent viscosity, and  $[\eta]$  has been evaluated from the relationship

$$[\eta] = 1.314 \times 10^{-2} M_w^{0.714} \quad (7)$$

given in ref 22. The values

$$\tau_1 = 2.05 \times 10^{-3} \text{ s (free draining)} \quad (8a)$$

$$\tau_1 = 1.4 \times 10^{-3} \text{ s (nondraining)} \quad (8b)$$

are obtained. That the latter model is the most adequate has earlier been shown by Jones and Caroline<sup>19</sup> and most recently by Nemoto et al.<sup>20,21</sup>

Figure 3 depicts data for the semidilute region where  $\bar{\Gamma}_f$  and  $\bar{\Gamma}_s$  are again resolved with eq 2 and  $\bar{\Gamma}_{cum}$  is obtained by the cumulant method. Both  $\bar{\Gamma}_f$  and  $\bar{\Gamma}_s$  are linear in  $q^2$ . The data for  $\bar{\Gamma}_s$  in the dilute and semidilute concentration intervals fit smoothly together as illustrated in Figure 4d. It is significant that this should be so since, if the bimodal character of the correlation function had been caused by dust or other supermolecular inhomogeneity, this would result in a slow relaxation of substantially lower frequency.

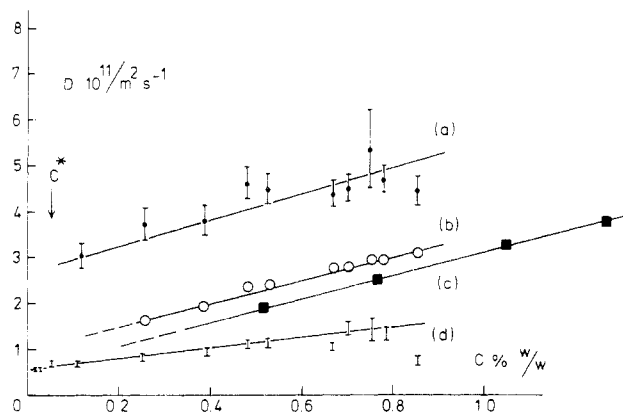


**Figure 4.** Concentration dependence of diffusion coefficients at low concentrations (PS ( $M = 8 \times 10^5$ ) in THF at 25 °C): (a) faster collective motions; (b) cumulant values; (c) classical gradient diffusion; (d) slow cooperative mode.

As noted earlier, inclusion of a base line term in conjunction with eq 2 (i.e., with a third exponential fixed at an infinite number of channels) resulted in its having a negligible amplitude in the fitting procedure.

The internal motions which were probed in the dilute region at  $qR > 1$  become above  $C^*$  indistinguishable from collective relaxations of the transient gel. This crossover behavior has been clearly demonstrated by quasi-elastic neutron scattering in the poly(dimethylsiloxane)/benzene system.<sup>35</sup>  $\bar{\Gamma}_f$  should thus correspond to the gel-mode coefficient,  $\bar{D}_c$ , in the range of wave vector employed here ( $qR = 1-4$ ). The choice of  $qR$  range is important since at  $qR \gg 1$  local motions of the structure will also be probed. However, the nonexponential character of the correlation function discussed here arises instead from admixture with a slow cooperative (see below) component rather than faster local segment motions (i.e., intramolecular motions). It is possible to ascertain the limiting angle above which local motions start to be significant from the  $D$  values evaluated by the method of cumulants. In the angular region utilized here,  $\bar{D}_{cum}$  is strictly angle independent. Similarly, the  $\Gamma$  vs.  $q^2$  plots are linear for both fast and slow components. It is, nevertheless, possible that internal modes do contribute to the fast mode, and their influence should become more pronounced as the concentration is decreased toward  $C^*$  and the modes become more difficult to separate. Figures 4 and 5 show the concentration dependences of fast ( $\bar{\Gamma}_f/q^2$ ) and slow ( $\bar{\Gamma}_s/q^2$ ) components, where the values at each concentration have been obtained as the slopes from linear plots such as those shown in Figure 3. Included in Figures 4 and 5 are values of  $\bar{D}_{cum}$  (cumulant evaluation), corresponding to the weighted average of the resolved fast and slow components. It is noted here that the method of cumulants is relevant only for unimodal distributions. Also shown are values  $\bar{D}_{CGD}$ , obtained by classical gradient diffusion. The faster mode is somewhat less well characterized than the slow since it is represented in relatively few channels. In the measurement interval, a log-log plot of the data for the faster mode gives 0.57 as the best value of the slope. This exponent is similar to that found<sup>12</sup> for intermediate molecular weights ( $\gamma = 0.59$ ) from measurements in a concentration range where only a single pseudogel mode is probed. The  $D$  values obtained as  $(\Gamma/q^2)$  have been corrected to a reference frame relative to the solvent velocity<sup>38</sup> using the factor  $(1 - \phi_p)$ , where  $\phi_p$  is the volume fraction polymer.

It is possible that the fast and slow modes are coupled to some extent, as their time scales become closer as  $C^*$  is approached. While the present data allow an adequate estimation of the concentration exponent, the main point

here being emphasized is that there are two coexisting gel modes where only one is anticipated from theory. The uncertainty associated with the data for the slower mode is lower. Here, a log-log plot leads to the relationship  $D_s \sim C^{0.44}$ . There is a significant trend noted for the  $D$  values to level out at the highest concentrations. As shown in Figures 4 and 5, the translational diffusion coefficient determined in dilute solution passes smoothly into the slower cooperative mode above  $C^*$ .

Schaefer and Han<sup>45</sup> in a recent review discuss the paucity of data supporting the scaling relationship:  $D_c \sim C^{0.75}$ , both as reflected in the scatter of the values of the reported exponent and also apparent changes in slope ("transitions") in log-log plots of  $D_c$  vs.  $C$  for various polymer-solvent systems, including PS/THF.

We suggest another possibility: the above may be a nearly trivial consequence of the almost universal presence of two gel modes in semidilute solutions coupled with data analysis by a method giving some average of these, for example with the cumulant method or with a single-exponential approximation. In such cases, since the relative weighting between the modes changes strongly with concentration (see Figure 6c)—the slower mode dominating close to  $C^*$  and the faster gel mode at  $C \gg C^*$ —the apparent exponent will be very sensitive to the particular range of concentration studied. A similar argument may be applied to exponents obtained using the classical gradient technique.

The classical gradient data give a corresponding exponent of 0.65. It was noted in a previous investigation<sup>12</sup> on fractions of lower molecular weight that this time-averaged quantity is intermediate between the fast and slow modes. This is so here and there is little evidence for identifying  $\bar{D}_{CGD}$  with either of these individual relaxations over at least most of the semidilute region. Although earlier workers<sup>30</sup> have used gradient diffusion to test scaling predictions, this must clearly be treated with reservation since most models necessarily are restricted to a specific mode of relaxation.

Only pseudogel motions were predicted to be probed in the  $qR$  interval 1-4 at concentrations substantially exceeding  $C^*$ . This does not seem to be the case at least for the very high molecular weight samples used here. For example, at the highest reduced concentration ( $C/C^* = 200$ ) the correlation function is still bimodal and the relative intensity contribution from the fast mode is about 0.85 (see Figure 6c). This finding conflicts with that of Adam and Delsanti,<sup>3</sup> who considered a single-exponential fit to be adequate when working in an identical region of  $qR/(C/C^*)$  space. On the other hand, these workers apparently did not make a comparative evaluation of other functions to their data. The present results fall into line with those of Chu and Nose<sup>4</sup> (PS/*trans*-decalin;  $\theta$  solvent) and Nishio and Wada<sup>6</sup> (PS/2-butanone; marginal), who have also investigated the dynamics of the semidilute region in a similar  $qR/(C/C^*)$  region. Both groups find bimodal autocorrelation functions (with a similar difference in relaxation rates) throughout the semidilute range on high molecular weight polystyrenes ( $M > 10^7$ ).

Chu and Nose<sup>4</sup> also comment the low  $\bar{\Gamma}_f \sim C^\gamma$  exponent in their system. Bimodal correlation functions may be expected in poor solvents<sup>24</sup> and indeed are predicted by Brochard.<sup>25</sup> However, in a good solvent it was anticipated that a uniform pseudogel would dominate the picture completely above  $C^*$ . Any slow motions would be expected<sup>37</sup> to derive from incipient reptative (nonisotropic) processes. Instead, we still observe a significant contribution to the scattered intensity from a slow cooperative mode having a positive concentration dependence as for

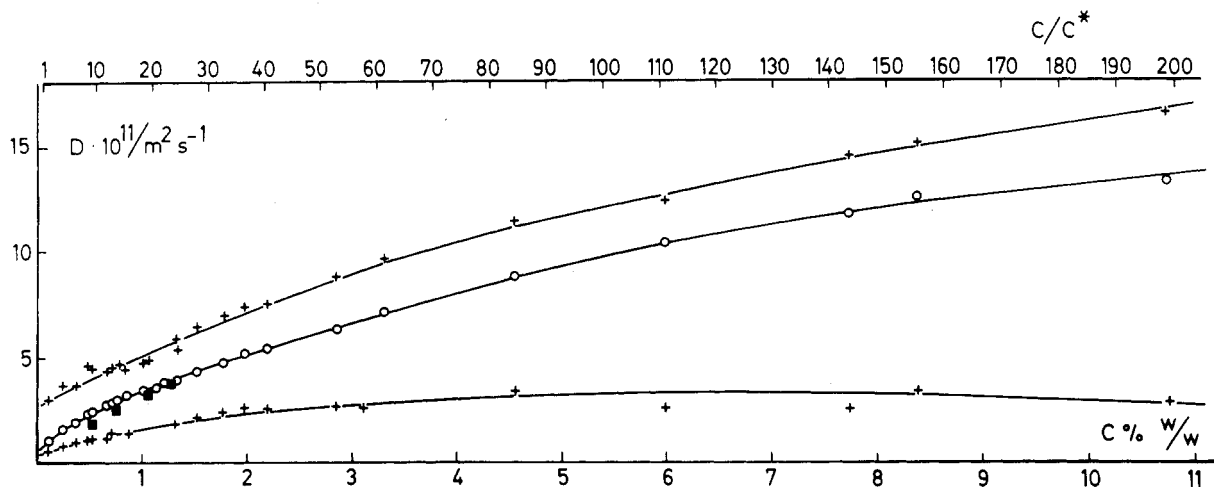


**Figure 5.** Concentration dependence of diffusion coefficients in the high-concentration range (PS ( $8 \times 10^6$ ) in THF at 25 °C). Points evaluated at each concentration as the slopes of linear plots illustrated in Figure 3. The legends to the curves are as in Figure 4.

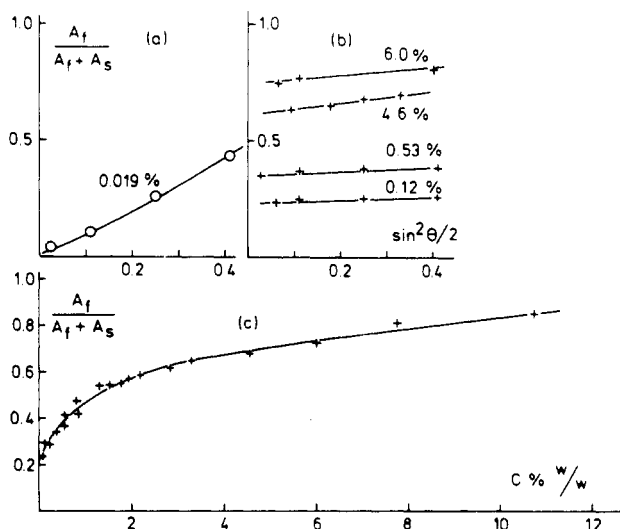


**Figure 6.** Variation of the relative intensity of scattering with  $\sin^2(\theta/2)$  and concentration for PS ( $M = 8 \times 10^6$ ) in THF: (a) intramolecular motions in the dilute region vs.  $\sin^2(\theta/2)$  ( $C = 0.021\%$ ); (b) faster collective motions as a function of angle at three semidilute concentrations; (c) faster cooperative mode shown as a function of concentration at a scattering angle of  $\theta = 40^\circ$  ( $C^* = 0.05\%$ ;  $C^* = 3M/4\pi R^3 N_A$ ).

translational motion in the dilute region.

We note here that the reduced osmotic pressure ( $\pi M/CRT$ ),<sup>26-28</sup> and hence the reduced osmotic compressibility, is a universal function of  $(C/C^*)$  above  $C^*$ , implying a unique static correlation length. The relationship between the latter and the dynamic length in a good solvent is not clearly established.<sup>29</sup> However, as follows from the above analysis, the presumption that only one characteristic dynamic length exists at semidilute concentrations in a good solvent is clearly incorrect and thus a conflict arises with the predicted behavior.<sup>1,3,25</sup> Only if the slower mode is also a cooperative phenomenon will there be justification for viewing the correlation length as a composite parameter involving the weighted average of the components (as is implicit in data evaluation using the cumulant method or a single-exponential approximation). To elucidate the dynamics of the system, however, requires models for the specific modes including their functional interrelationship. Comparisons of the dynamic data with the static screening length<sup>3</sup> or the fictive tube formed by the entanglement spacing<sup>39</sup> are premature if two substantially different gel modes are simultaneously detected in the dynamic experiment.

The fraction of the scattered intensity due to the fast mode in the dilute and semidilute regions is shown as a function of  $q^2$  in Figure 6a,b. In dilute solution (Figure 6a) at the lowest angles ( $\theta \leq 20^\circ$ ), where the sufficient condition  $qR < 1$  is met, the autocorrelation function is a single exponential. With increasing angle there is a marked increase in the contribution to the intensity from intramolecular motions and the correlation functions are then bimodal. Such behavior agrees qualitatively with theory but, as shown by Nemoto et al.,<sup>20,21</sup> in good solvents, the data are less well described by these relationships than those in poor solvents.

In the semidilute region (Figure 6b) the fraction of the scattered intensity ascribable to pseudogel motions changes only slowly with  $q^2$ . A similar observation has been made by Chu and Nose<sup>4</sup> and Nishio and Wada.<sup>6</sup> The correlation function was thus found to be consistent with a bimodal function even at the lowest angles. This is so since the condition  $qR \ll 1$  must be fulfilled according to ref 1 before the slower mode can be isolated alone and this is not realizable with such a high molecular weight sample as used here.

The relative intensity contribution of the fast mode is shown as a function of concentration for data at a measuring angle of  $40^\circ$  in Figure 6c. It is shown here that at the highest reduced concentration used ( $C/C^* = 200$ ) the fraction is about 0.85. Although it is often tempting to assign multiexponential behavior to the presence of dust or other inhomogeneities, the systematic trends in the present data effectively discount this. For example, the increase in the relative amplitude of the faster mode with concentration is inconsistent with the presence of extraneous scatterers, since the slow mode would then be the one to increase.

There is always the possibility that some mechanical degradation has occurred during preparation/filtration of the solutions. However, since the semidilute solutions with bimodal correlation functions gave monomodal correlation functions at low angle when diluted to the dilute region, this appears unlikely. Another possibility is that the method of data analysis introduces artifacts. For this reason we have performed an extensive series of simulations.<sup>12,31</sup> Normally distributed pseudorandom numbers of a size typical of the residuals in a real run were added to "experiments" constructed by using parameter values covering the range in the actual runs. It was found that the parameter estimates from the fitting procedure are "true" values without significant bias. Even when the minor component represents only 7% of the total, this

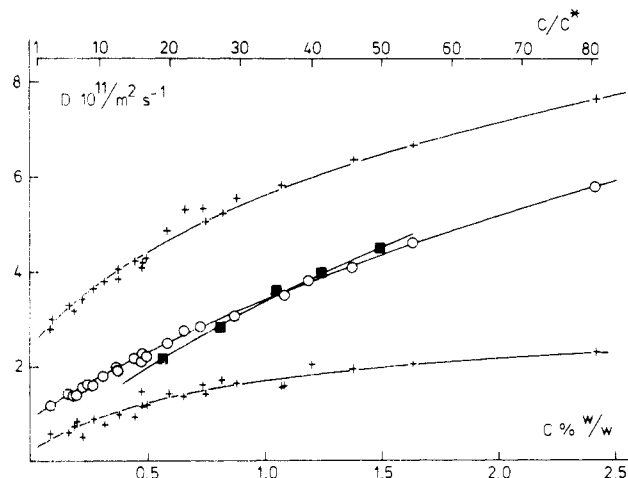


**Figure 7.** Concentration dependence of the diffusion coefficients for PS  $M = 15 \times 10^6$  in THF at 25 °C. Details are as given in Figure 5. Data at an angle of 40° corresponding to  $qR_G \approx 3.3$  ( $C^* = 0.03\%$ ).

mode can be consistently separated and well defined if the relaxation times differ by at least a factor of 1.3. This latter condition is difficult to fulfill for example in poor solvents and as  $C \rightarrow C^*$ . It is not suggested that complete separation of the two modes has been achieved by the present routines and eq 2. Alternative methods may give improved separation and better resolution of the pseudogel component. There are inherent features of the problem which must be considered, however, regardless of the sophistication of the procedure used. For example, while the slow mode is represented in all channels the fast occupies progressively fewer with increasing concentration and if an optimum sampling time is used to include both relaxations in the experiment, the precision of the fast mode diminishes. Also, with decreasing concentration, the relaxation times of the modes approach each other and separation becomes increasingly difficult as the average frequencies ( $\bar{\Gamma}$ ) begin to overlap. The present approach does, however, serve to demonstrate the complexity of semidilute solution dynamics, which evidently still constitute an ill-characterized field. The bimodal fit used here is only the most simple of possible alternatives which may be equally consistent with the data. The present approach involves the assumption of the number of relaxation processes involved. An alternative is the use of a program such as CONTIN<sup>42,43</sup> introduced by Provencher which requires only the autocorrelation function and the range of possible relaxation times. However, analysis of simulated experiments and also mixtures of various monodisperse polymers in different proportions, revealed that this latter approach, while more appealing in principle, gives a significantly poorer resolution of the relaxation times when these approach each other (i.e., less than a factor of 2). The nature of the present system involves relaxations which approach each other as the concentration falls toward  $C^*$ . Also the expectation from current semidilute solution theory is that only a small number of relaxations may be present; i.e., above but still close to  $C^*$  there will be a gel mode and a translational component. For these reasons, the present approach is deemed more pragmatic here.

Measurements on the fraction with  $M = 8 \times 10^6$  have been complemented with data for a fraction of higher molecular weight ( $M = 15 \times 10^6$  and extending up to value of  $C/C^* \approx 80$ ). The angular region is again restricted so that the bounds referred to in the Introduction are satisfied.

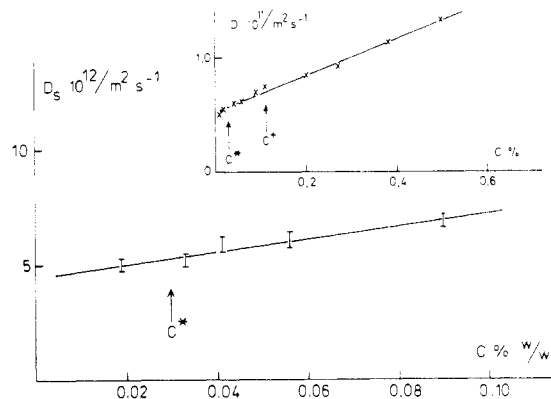


**Figure 8.** Data for PS ( $M = 15 \times 10^6$ )/THF at dilute concentrations by measurements at low angle ( $\theta = 20^\circ$ ). The insert shows the same data together with those for semidilute concentrations isolated as the slow, cooperative mode, using bimodal analysis. ( $C^* = M/R^3 N_A$ ).

The results for this sample are summarized in Figure 7 and are broadly similar to those for the lower molecular weight sample (Figure 5). Within experimental uncertainty, both modes resolved in semidilute solution are independent of molecular weight and are thus viewed as cooperative in character.

The measurements on PS 15M have been extended down to the dilute region (Figure 8). These data have been obtained at low angles ( $\theta \leq 20^\circ$ ) where only the translational mode is represented in the time correlation function. The observation that the latter is strictly a single exponential at low concentration and at low angles shows that the significant polydispersity of this fraction ( $M_w/M_n \approx 1.3$ ) does not complicate the resolution into the two modes as illustrated in Figure 7. The compatibility of the slower mode data in semidilute solution, derived from eq 2, with those for translational diffusion in dilute solution is shown in the insert to Figure 8.

de Gennes' theory<sup>1</sup> has, of course, been of great conceptual value for aiding our understanding of semidilute solutions. It seems, however, to represent an oversimplification of the dynamics of real systems. It has been generally accepted that the simple power laws derived therein will be valid in the limit of very high molecular weight. The low values of the exponent in  $D \sim C^\gamma$  for the present samples in comparison with the predicted value of 0.75 for the pseudogel are thus relevant. Intermediate molecular weights ( $M \sim 10^6$ ) in good solvents at high monomer concentration in fact approach the theoretical value more closely ( $\gamma \approx 0.6$ )<sup>3,11,12</sup> and are also characterized by correlation functions more closely approximating a single exponential. Small coils are often studied at high monomer concentrations giving extensive coil interpenetration and thus have an approximately homogeneous monomer distribution as is presumed to exist above  $C^*$  and to be maintained as the segment density increases uniformly with concentration. Very large coils, on the other hand, are generally investigated at concentrations giving only limited coil interpenetration and thus the data may fail to meet the assumptions on which scaling theory rests. Qualitatively, one may speculate that the partially overlapping and interpenetrating coils, forming part of the same overall (but not homogeneous) network, could be expected to display two modes: the anticipated gel mode from nonoverlapping regions and the slower mode related to the relaxation of the overlapping entanglement regions. That the slow mode derives from such a source in the case of very large coils seems more credible than hydrodynamic

motions since these should be extremely slow at the concentrations used here and also strongly dependent on molecular weight, neither of which are observed. It may be added that recent measurements of polymer self-diffusion<sup>29</sup> in the semidilute region in good solvents do not support de Gennes' predicted concentration dependence. The same is true for the concentration dependence of the sedimentation coefficient. Taken together the various indices suggest a fundamental weakness in the models used.

Bimodal analysis and the method of cumulants are alternative approaches to data analysis. One reason for preferring the former is the following: at concentrations well above  $C^*$  it is possible to roughly estimate the slow component as a single exponential by choosing a sufficiently long sampling time that the fast mode has decayed completely within the first few channels. (However, the fast component cannot be similarly isolated using a very short sampling time.) Indirect evidence supporting the multimodal alternative is the collinearity of the slow component at semidilute concentrations with the translational diffusion coefficient obtained as a single exponent in dilute solution at low angles. However, evidence from a complementary source is needed and this has recently appeared. Subsequent to submission of this paper, Koberstein et al.<sup>44</sup> described elastic light and neutron scattering experiments on semidilute polystyrene solutions. They concluded that a single length scale is inadequate to describe the scattering behavior both in good and  $\Theta$  solvents. A second correlation length is necessary to describe the solution structure and which is comparable to the radius of gyration of the dissolved polymer. A tentative explanation was posed in terms of limited chain interpenetration effects.

## Conclusions

The semidilute region is, in general, characterized by nonexponential autocorrelation functions for large coils in a good solvent. It is possible to resolve the latter into fast and slow components in an internally consistent manner, both modes being cooperative in character and reflecting the heterogeneity of the transient gel. The general presence of more than one mode is seldom adequately recognized. Instead, most data treatment is confined to the use of the average quantity obtained by cumulant analysis. While a number of routines of varying sophistication have been used to resolve multiexponential functions and, a comparison of their relative utility is lacking, it is anticipated that such an approach will eventually prove to be adequate for testing pseudogel theory. More detailed theoretical models are required to describe the dynamical behavior of very large coils at higher concentrations. Comparisons with the independent classical measurements of diffusion have been made, but it is unlikely that these can be meaningfully used to test scaling theory for a specific mode.

**Registry No.** Polystyrene, 9003-53-6; THF, 109-99-9.

## References and Notes

- (1) (a) de Gennes, P.-G. *Macromolecules* **1976**, *9*, 587, 594. (b) de Gennes, P.-G. "Scaling Concepts in Polymer Physics"; Cornell University Press: London, 1979.
- (2) Daoud, M.; Cotton, J. P.; Farnoux, B.; Jannink, G.; Sarma, G.; Benoit, H.; Duplessix, R.; Picot, C.; de Gennes, P.-G. *Macromolecules* **1975**, *8*, 804.
- (3) Adam, M.; Delsanti, M. *Macromolecules* **1977**, *10*, 1229.
- (4) (a) Nose, I.; Chu, B. *Macromolecules* **1979**, *12*, 590, 599. (b) Chu, B.; Nose, I. *Macromolecules* **1980**, *13*, 122.
- (5) Yu, T. L.; Reihanian, H.; Jamieson, A. M. *Macromolecules* **1980**, *13*, 1590.
- (6) Nishio, I.; Wada, A. *Polym. J.* **1980**, *12*, 145.
- (7) Munch, J.-P.; Herz, J.; Boileau, S.; Candau, S. *Macromolecules* **1981**, *14*, 1370.
- (8) Munch, J.-P.; Hild, G.; Candau, S. J. *Macromolecules* **1983**, *16*, 71.
- (9) Mathiez, P.; Mouttet, C.; Weisbuch, G. *J. Phys. (Paris)* **1980**, *41*, 519.
- (10) Mathiez, P.; Weisbuch, G.; Mouttet, C. *Biopolymers* **1979**, *18*, 1465; **1981**, *20*, 2381.
- (11) Selser, J. C. *J. Chem. Phys.* **1983**, *79* (2), 1044.
- (12) Brown, W.; Johnsen, R. M. *Macromolecules* **1985**, *18*, 379.
- (13) Amis, E.; Han, C. C. *Polymer* **1982**, *23*, 1403.
- (14) Amis, E.; Han, C. C.; Matsushita, Y. *Polymer* **1984**, *25*, 650.
- (15) Koppel, D. E. *J. Chem. Phys.* **1972**, *57*, 4814.
- (16) Jamieson, A. M.; Venkataswamy, K. *Polym. Bull.* **1984**, *12*, 275.
- (17) Pecora, R. *J. Chem. Phys.* **1964**, *40*, 1604; **1965**, *43*, 1562; **1968**, *49*, 1032.
- (18) Huang, W. N.; Frederick, J. E. *Macromolecules* **1974**, *7*, 34.
- (19) Jones, G.; Caroline, D. *Chem. Phys.* **1979**, *37*, 187; **1979**, *40*, 153.
- (20) Tsunashima, Y.; Nemoto, N.; Kurata, M. *Macromolecules* **1983**, *16*, 584, 1184.
- (21) Nemoto, N.; Makita, Y.; Tsunashima, Y.; Kurata, M. *Macromolecules* **1984**, *17*, 425.
- (22) Meyerhoff, G.; Appelt, B. *Macromolecules* **1979**, *12*, 968.
- (23) Wells, J. J. *Chem. Soc., Faraday Trans. 1* **1984**, *80*, 1233.
- (24) Adam, M.; Delsanti, M. *J. Phys. (Paris), Lett.* **1984**, *45*, L-279.
- (25) Brochard, F. *J. Phys. (Paris)* **1983**, *44*, 39.
- (26) Noda, I.; Kato, N.; Kitano, T.; Nagasawa, M. *Macromolecules* **1981**, *14*, 668.
- (27) Higo, Y.; Ueno, N.; Noda, I. *Polym. J.* **1983**, *15*, 367.
- (28) Noda, I.; Higo, Y.; Ueno, N.; Fujimoto, T. *Macromolecules* **1984**, *17*, 1055.
- (29) Callaghan, P. T.; Pinder, D. N. *Macromolecules* **1984**, *17*, 431.
- (30) Roots, J.; Nyström, B. *Macromolecules* **1980**, *13*, 1595.
- (31) Johnsen, R. Proceedings of the 27th Microsymposium on Macromolecules, Prague, 1984.
- (32) Marquardt, D. W. *SIAM J. Appl. Math.* **1963**, *11*, 431.
- (33) Zimm, B. H. *J. Chem. Phys.* **1956**, *24*, 269.
- (34) Rouse, P. E. *J. Chem. Phys.* **1953**, *21*, 1272.
- (35) Ewen, B.; Richter, D.; Hayter, J. B.; Lehner, B. *J. Polym. Sci., Polym. Lett. Ed.* **1982**, *20*, 233.
- (36) Patterson, G. D.; Jarry, J.-P.; Lindsey, C. P. *Macromolecules* **1980**, *13*, 668.
- (37) Hwang, D.-h.; Cohen, C. *Macromolecules* **1984**, *17*, 1679.
- (38) Geissler, E.; Hecht, A. M. *J. Phys. (Paris), Lett.* **1979**, *40*, L-173.
- (39) Nemoto, N.; Makita, Y.; Tsunashima, Y.; Kurata, M. *Macromolecules* **1984**, *17*, 2629.
- (40) Adam, M.; Delsanti, M. *J. Phys. (Paris)* **1980**, *41*, 713.
- (41) Sun, S. T.; Nishio, I.; Swislow, G.; Tanaka, T. *J. Chem. Phys.* **1980**, *73*, 5971.
- (42) Provencher, S. W.; Hendrix, J.; De Maeyer, L.; Paulussen, N. *J. Chem. Phys.* **1978**, *69*, 4273.
- (43) Provencher, S. W. *Makromol. Chem.* **1979**, *180*, 201.
- (44) Koberstein, J. T.; Picot, C.; Benoit, H. *Polymer* **1985**, *26*, 673.
- (45) Schaefer, D. W.; Han, C. C. In "Dynamic Light Scattering"; Pecora, R., Ed.; Plenum: New York, 1985.